Magnetic Resonance in Medicine 62:739–746 (2009)

General Formulation for Quantitative G-factor Calculation in GRAPPA Reconstructions

Felix A. Breuer,[1*] Stephan A.R. Kannengiesser,[2] Martin Blaimer,[1] Nicole Seiberlich,[3] Peter M. Jakob,[1,4] and Mark A. Griswold[3]

In this work a theoretical description for practical quantitative estimation of the noise enhancement in generalized autocalibrating partially parallel acquisitions (GRAPPA) reconstructions, equivalent to the geometry (g)-factor in sensitivity encoding for fast MRI (SENSE) reconstructions, is described. The GRAPPA g-factor is derived directly from the GRAPPA reconstruction weights. The procedure presented here also allows the calculation of quantitative g-factor maps for both the uncombined and combined accelerated GRAPPA images. This enables, for example, a fast comparison between the performances of various GRAPPA reconstruction kernels or SENSE reconstructions. The applicability of this approach is validated on phantom studies and demonstrated using in vivo images for 1D and 2D parallel imaging. Magn Reson Med 62: 739–746, 2009. © 2009 Wiley-Liss, Inc.

Key words: GRAPPA; g-factor; parallel imaging; quantitative noise enhancement

The signal-to-noise ratio (SNR) is the dominating limiting factor in MRI. In recent years the advent of multicoil arrays has offered the possibility to significantly increase the intrinsic SNR in an image; however, this increase is at the expense of nonuniform SNR in the final images (1). In addition, both the increased sensitivity and the encoding capability of modern multicoil arrays has opened the door for parallel MRI (pMRI), which is associated with significant scan time reductions in many clinical applications. However, pMRI reconstruction methods such as sensitivity encoding for fast MRI (SENSE) (2), simultaneous acquisition of spatial harmonics (SMASH) (3), and generalized autocalibrating partially parallel acquisitions (GRAPPA) (4) also come with a nonuniform loss in SNR compared to nonaccelerated images. In general, the SNR after parallel imaging reconstruction is decreased by the square root of the reduction factor R as well as by an additional coil-geometry dependent factor. This second factor, known as geometry (g)-factor in the parallel imaging community, results in a spatially variant noise enhancement that strongly depends on the reduction factor and the encoding capability of the receiver array. Analytical approaches for determining this geometry factor for SENSE (2) and SMASH (5) reconstructions have already been derived. Both have been used to complement the reconstructions in SNR units proposed by Kellman and McVeigh (6). In addition, Yeh et al. (7) presented a general framework for calculating the g-factor in PARS reconstructions.

In recent years several approaches have been described to estimate the nonuniform noise enhancement in GRAPPA reconstructions (8–10). However, a practical analytical description for a quantitative GRAPPA g-factor has not yet been derived.

The gold standard method for estimation of the spatially varying noise enhancement is to acquire a fully encoded series of images with identical parameters. Out of this image series an SNR map of the fully encoded image can be derived by taking the mean and the standard deviation on a pixel-by-pixel basis throughout the image series. An accelerated experiment for each image in the series can be mimicked by skipping a portion of the *k*-space phase encoding lines. After subsequent GRAPPA reconstruction of all retrospectively accelerated images in the series, a GRAPPA accelerated SNR map can be calculated as in the fully encoded case. The nonuniform noise enhancement due to the GRAPPA reconstruction can then be derived on a pixel-by-pixel basis by dividing the fully encoded SNR map by the GRAPPA SNR map and the square root of the acceleration factor. In order to provide accurate results using this method, at least 100 images are required. As can be imagined, this method is very time-consuming since at least 100 fully encoded experiments and 100 GRAPPA reconstructions have to be performed for accurate SNR estimation. In addition, this approach is only applicable to static imaging scenarios. Recently proposed methods, such as the pseudomultiple replica SNR measurement (10,11), allow the calculation of SNR maps by acquiring only one fully encoded image and an additional noise-only dataset, and thus is also appropriate for applications on moving objects. However, these methods are still time-consuming because at least 100 separate image reconstructions are necessary for accurate results.

In this work a general framework for quantitative estimation of the spatially varying noise enhancement in GRAPPA reconstructions is described. The presented method works by calculating the GRAPPA-related noise enhancement directly from the GRAPPA reconstruction weights for both uncombined single coil GRAPPA images as well as combined images (e.g., sum of squares [SOS] or B1 normalized). In addition, it is demonstrated that the framework presented here is also applicable to imaging scenarios where multiple GRAPPA kernels are employed, such as in variable density (12) and non-Cartesian GRAPPA (13–16).

[1]Research Center Magnetic Resonance Bavaria (MRB), Würzburg, Germany.
[2]Siemens Medical Solutions, Erlangen, Germany.
[3]Department of Radiology, University Hospitals of Cleveland, Cleveland, Ohio.
[4]Department of Experimental Physics 5, University of Würzburg, Germany.
Grant sponsor: Bavarian Ministry of Economic Affairs and Technology (BayStMWIVT).
*Correspondence to: Dr. Felix Breuer, Research Center, Magnetic Resonance Bavaria (MRB), Am Hubland, D-97074 Würzburg, Germany. E-mail: breuer@mr-bavaria.de
Received 17 June 2008; revised 27 March 2009; accepted 2 April 2009.
DOI 10.1002/mrm.22066
Published online 7 July 2009 in Wiley InterScience (www.interscience.wiley.com).

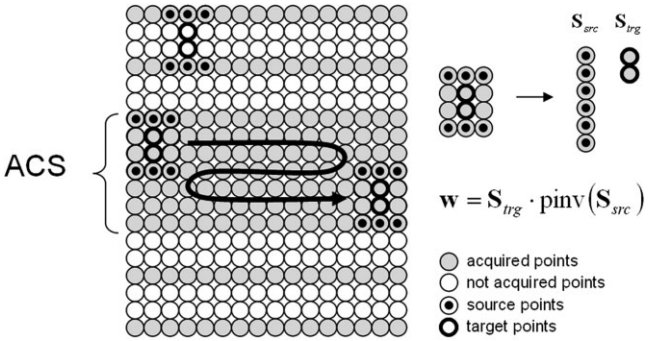

FIG. 1. Schematic description of GRAPPA weights determination: According to the undersampling scheme (here R = 3), a GRAPPA reconstruction kernel is defined (here 2 × 3) in which source and target points are identified (coil dimension omitted). The kernel is slid through the ACS data and all the kernel repetitions are collected in a source matrix $\mathbf{S}_{src}$ and target matrix $\mathbf{S}_{trg}$. The GRAPPA reconstruction weights are then derived by solving Eq. [1].

The GRAPPA reconstruction procedure is normally performed in *k*-space as a convolution of the GRAPPA weights with the undersampled *k*-space data. However, by exploiting the convolution theorem GRAPPA can also be reinterpreted in image space and thus formulated as a pixel-by-pixel matrix multiplication of GRAPPA weights in image space with the folded (undersampled) multicoil images (8,17). It will be shown that the GRAPPA reconstruction formalism in image space can be useful when analyzing the noise propagation into the final GRAPPA reconstruction. It is also demonstrated that it is essential to take potential noise correlations into account when calculating the GRAPPA g-factors for accurate results. Both 2D phantom and 3D in vivo results demonstrate the accuracy and general applicability of this approach.

THEORY

In the following section a short review of the GRAPPA reconstruction procedure is given. Before the actual GRAPPA reconstruction can be performed a GRAPPA reconstruction weight set has to be derived. These GRAPPA weights are typically derived in *k*-space from a low-resolution fully encoded autocalibration (ACS) dataset with sufficient SNR.

Weights Determination in GRAPPA

In the first step the GRAPPA kernel source and target points are identified according to the reduced sampling scheme used (e.g., R = 3, 2 × 3 kernel) as depicted in Fig. 1. In a second step the reconstruction kernel is slid through the ACS data and the source and target points for all available kernel repetitions N_{rep} are assembled into a source matrix $\mathbf{S}_{\mathrm{src}}$ (size: $N_c \cdot N_{src} \times N_{rep}$) and a target matrix $\mathbf{S}_{\mathrm{trg}}$ (size: $N_c \cdot N_{trg} \times N_{rep}$). In a third step, the reconstruction weights $\mathbf{w}$ (size: $N_c \cdot N_{trg} \times N_c \cdot N_{src}$) are derived by solving Eq. [1] for the reconstruction weight set $\mathbf{w}$ via the Moore–Penrose pseudoinverse.

$$\mathbf{w} \cdot \mathbf{S}_{src} = \mathbf{S}_{trg} \qquad [1]$$

Since the GRAPPA weights are derived from a low-resolution dataset with sufficient SNR and a sufficient number of kernel repetitions within the ACS the weights can be considered "noise free." Similar to the smoothing/denoising/fitting algorithm employed in the coil mapping procedure for SENSE reconstructions the Moore–Penrose Pseudoinverse (least-square fit) ensures accurate "noise-free" weights in the GRAPPA reconstruction.

GRAPPA Reconstruction Weights

Once the weight set $\mathbf{w}$ has been derived, the missing $N_{trg} = R\text{-}1$ data points in each coil (not acquired data) can be calculated by applying the weight set $\mathbf{w}$ to the acquired undersampled dataset. In order to arrive at the GRAPPA-accelerated fully encoded *k*-space signal S^{acc} this procedure is repeated for each acquired point in the reduced *k*-space signal S^{red}.

Thus, GRAPPA can also be seen as a convolution procedure of the acquired reduced *k*-space signal S_l^{red} with a GRAPPA convolution kernel w_{kl} where k and l run from 1 to the number of coils N_c in the receiver array. The convolution kernel is made up of the GRAPPA weight set from Eq. [1] as schematically depicted in Fig. 2.

$$S_k^{acc} = \sum_{l=1}^{N_c} S_l^{red} \otimes w_{kl} \qquad [2]$$

The convolution theorem states that this convolution process in *k*-space can also be formulated in image space

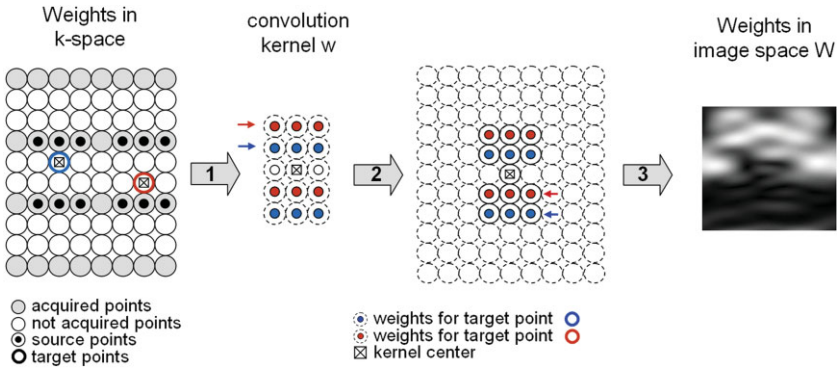

FIG. 2. Determination of GRAPPA weights in image space (coil dimensions are omitted): Step 1: The GRAPPA reconstruction weights in *k*-space for each target point (blue and red) are reordered to build a convolution kernel in *k*-space with a mutual kernel center. Step 2: The convolution kernel in *k*-space is flipped in both dimensions (indicated by arrows) and zero-padded to the final image size (N_y,N_x). Step 3: Inverse 2D Fourier transformation of zero-padded, flipped convolution kernel to derive the GRAPPA weights in image space.

by applying a two-dimensional inverse Fourier transformation to Eq. [2]. The accelerated GRAPPA image in the k-th coil I_k^{acc} is then simply given by a pixel-by-pixel multiplication of the GRAPPA weights in image space W_{kl} with the folded coil images I_l^{red} (8). Using the properties of the convolution theorem, the W_{kl} can be derived by 2D inverse Fourier transformation of the convolution kernel w_{kl} in *k*-space.

$$I_k^{acc} = \sum_{l=1}^{N_c} W_{kl} \cdot I_l^{red} \quad [3]$$

A schematic description of the practical implementation of GRAPPA in the image domain is given in Fig. 2. In Eq. [2], the GRAPPA weights in *k*-space can be seen to contain also the weights that will transform the acquired data untouched. Thus, these weights are 0 for all points in the kernel except for the points that are transformed untouched. These weights have value 1. This corresponds to setting the kernel center to 1 when calculating the weights in image space (see Fig. 2). The mathematics given in Eqs. [2] and [3] are simplified in order to provide a practical and comprehensive analytical instruction of GRAPPA in image space. However, in Ref. (17) a more complete mathematical description of viewing GRAPPA as a multiplication in image space can be found.

Noise Propagation in GRAPPA Reconstructions

In order to investigate how the acquired noise propagates into the accelerated GRAPPA images the GRAPPA representation in the image domain (Eq. [3]) is examined and the variances $\sigma^2(I_k^{acc})$ of the GRAPPA reconstructed single coil images I_k^{acc} are determined. In order to simplify the process, in the following considerations the noise term is separated from the signal and Eq. [3] yields:

$$I_k^{acc} + n_k^{acc} = \sum_{l=1}^{N} W_{kl} \cdot (I_l^{red} + n_l^{red}) \quad [4]$$

The noise-free signal terms cancel when calculating the variances of the GRAPPA single coil images and only the variance of a weighted sum of noise contributions remain. Thus, the variance of the accelerated GRAPPA images can be written as:

$$\sigma^2(n_k^{acc}) = \sigma^2\left(\sum_{l=1}^{N} W_{kl} \cdot n_l^{red} \right) = \sum_{l=1}^{N} |W_{kl}|^2 \cdot \sigma^2(n_l^{red}) + 2 \sum_{l=1}^{N} \sum_{m=l+1}^{N} |W_{kl} W_{km}| \cdot \sigma^2(n_l^{red}, n_m^{red}) \quad [5]$$

In this equation $\sigma^2(n_l^{red}) = \sigma^2{}_{ll}$ represents the noise variance in channel *l* and $\sigma^2(n_l^{red}, n_m^{red}) = \sigma^2{}_{lm}$ the noise covariance between channel *l* and *m*. Eq. [5] can greatly be simplified when switching to matrix notation. Introducing the GRAPPA weights matrix $\mathbf{W}$ in image space and the noise covariance matrix $\mathbf{\Sigma}^2$

$$W = \begin{pmatrix} W_{11} & \cdots & W_{1N} \\ \vdots & \ddots & \vdots \\ W_{N1} & \cdots & W_{NN} \end{pmatrix} \quad \text{and} \quad \sum^2 = \begin{pmatrix} \sigma_{11}^2 & \cdots & \sigma_{1N}^2 \\ \vdots & \ddots & \vdots \\ \sigma_{N1}^2 & \cdots & \sigma_{NN}^2 \end{pmatrix} \quad [6]$$

Eq. [5] calculates to:

$$\sigma^2(n_k^{acc}) = \sigma^2\left(\sum_{l=1}^{N} W_{kl} \cdot n_l^{red} \right) = |\mathbf{W} \cdot \Sigma^2 \cdot \mathbf{W}^H|_{kk} \quad [7]$$

In this equation H denotes the transpose complex conjugate of a matrix. Taking into account that the variance of the fully encoded k-th coil image I_k^{full} is reduced by the acceleration factor R the variance of the fully encoded image is given by:

$$\sigma^2(n_k^{full}) = \frac{1}{R} \cdot \sigma_{kk}^2 = \frac{1}{R} \cdot |\Sigma^2|_{kk} \quad [8]$$

Thus, similar to the g-factor definition known from SENSE-type reconstructions:

$$g = \frac{SNR_{full}}{SNR^{acc} \cdot \sqrt{R}} \quad [9]$$

the GRAPPA g-factor for the k-th coil image can be derived:

$$g_k = \frac{SNR_k^{full}}{SNR_k^{acc} \cdot \sqrt{R}} = \frac{\sigma(n_k^{acc})}{\sigma(n_k^{full}) \cdot \sqrt{R}} = \frac{\sqrt{|\mathbf{W} \cdot \Sigma^2 \cdot \mathbf{W}^H|_{kk}}}{\sqrt{|\Sigma^2|_{kk}}} \quad [10]$$

Although the single coil GRAPPA g-factor directly represents the noise enhancement resulting from the GRAPPA reconstruction, it is important to derive also a GRAPPA g-factor for combined images. It is important to note that the g-factor becomes also a function of the coil combining algorithm. Considering the image combination as a linear combination of the single coil images,

$$I_{comb}^{acc} = \sum_{k=1}^{N} p_k \cdot I_k^{acc} = \sum_{k=1}^{N} p_k \cdot \sum_{l=1}^{N} W_{kl} \cdot I_l^{red} \quad [11]$$

a g-factor for combined GRAPPA images can be derived similar to the considerations above:

$$g_{comb} = \frac{SNR_{comb}^{full}}{SNR_{comb}^{acc} \cdot \sqrt{R}} = \frac{\sqrt{|(\mathbf{p}^T \cdot \mathbf{W}) \cdot \Sigma^2 \cdot (\mathbf{p}^T \cdot \mathbf{W})^H|}}{\sqrt{|(\mathbf{p}^T \cdot 1) \cdot \Sigma^2 \cdot (\mathbf{p}^T \cdot 1)^H|}} \quad [12]$$

The coefficients p_k in the vector $\mathbf{p}$ can simply be determined either from the low-resolution ACS data or the high-resolution accelerated GRAPPA images. In the case of an SOS reconstruction, these coefficients are given by $p_k = I^*_k / I_{SOS}$ (8). Roemer et al. (1) have shown that the SOS-image combination represents a near SNR optimal image reconstruction without the need of extra knowledge of the coil sensitivity profiles. An SNR-optimal image combination, however, requires the knowledge of the coil sensitivity profiles for both nonnormalized and B1-normalized image combination. The difference between both combination methods is just a scalar scaling factor for each image pixel that depends only on the coil sensitivities. However, since the GRAPPA g-factor is given in relation to the fully encoded image SNR on a pixel-by-pixel basis this scaling factor cancels out in Eq. [12]. Therefore, the GRAPPA

g-factors for nonnormalized and B1-normalized image reconstruction with optimal SNR are identical and the SOS-GRAPPA g-factor can be considered an accurate estimate for basically all commonly used combining methods.

So far, the framework presented here has been described for scenarios where only a single GRAPPA weight-set was used for image reconstruction (conventional Cartesian GRAPPA for 2D and 3D imaging). However, the concept described here can be extended to more complicated GRAPPA applications where multiple GRAPPA weight sets are required or the ACS data is included in the final reconstruction. Each time a certain kernel is applied in *k*-space the noise propagates according to Eq. [7] into the image independent from the location where the kernel has been applied. This concept is applicable even in the case of shared source points at the border between multiple kernels. Thus, when analyzing the noise propagation after application of multiple GRAPPA kernels (or included ACS data) the variance for each GRAPPA kernel according to Eq. [7] must be determined and weighted with the fraction of *k*-space to which the kernel has been applied. One can show that for the final g-factor calculation the g-factor for each GRAPPA kernel can be determined (Eq. [10] for uncombined, Eq. [12] for combined g-factor) and weighted with the corresponding reduction factor R_m and the fraction f_m of *k*-space in which the specific kernel has been applied. Thus, in general the effective g-factor (g_{eff}) for GRAPPA reconstructions with multiple kernels or included ACS data ($R_1 = 1$, $g_1 = 1$, f_1 = number of ACS lines/total number of lines in fully encoded *k*-space) calculates to:

$$g_{eff} = \sqrt{\sum_{m=1}^{N} f_m \cdot R_m \cdot g_m^2}/R_{eff} \quad \text{with } R_{eff} = \left(\sum_{m=1}^{N} \frac{f_m}{R_m}\right)^{-1} \qquad [13]$$

MATERIALS AND METHODS

All experiments were performed on a 1.5T clinical Scanner (Avanto, Siemens Medical Solutions, Erlangen, Germany) equipped with a 12-channel head coil array for signal reception. Image reconstructions, g-factor calculations and analyses were performed offline using the MatLab programming environment (MathWorks, Natick, MA).

Phantom Experiments

In order to provide an accurate reference for g-factor analysis, a fully encoded phantom image was acquired with following parameters: TE/TR = 7.1/40 ms, $\alpha = 30°$, bw = 100 Hz/px, FOV = 210 × 210 mm², matrix = 256 × 256. To allow for a correction of the noise correlations between the individual receiver channels, an additional noise-only image ($\alpha = 0°$) was acquired with identical imaging parameters. Various accelerated (R = 2, 3 and 4) GRAPPA acquisitions were mimicked by removing the corresponding phase-encoding steps retrospectively. For the fully encoded image and each acceleration scenario, an artificial image series was generated using the pseudomultiple replica approach as described below. The GRAPPA weights were derived in *k*-space as described in Fig. 1 using a 4 × 5 kernel and 32 × 32 ACS block.

In Vivo Experiments

In addition to the 2D phantom experiments a fully encoded 3D in vivo axial MPRAGE (magnetization prepared rapid gradient echo) head experiment was performed on a volunteer and informed consent was obtained prior to the acquisition. The following sequence parameters were used: TE/TR = 4.38/1350 ms, TI = 800 ms, $\alpha = 15°$, bw = 180 Hz/px, FOV = 250 × 187 × 160 mm³, matrix = 256 × 192 × 160. Rectangular (R = 2 × 2) and CAIPIRINHA-type (R = 2 × 2(1)) (18) accelerated acquisitions were mimicked by removing the corresponding phase-encoding steps. The GRAPPA reconstructions were performed with a 3D GRAPPA kernel according to the 2D undersampled phase-encoding scheme. In both cases the kernel size was 3 × 3 × 3 and a 24 × 24 × 32 ACS block was used. The GRAPPA weights were derived in *k*-space as schematically depicted in Fig. 1 for a 2D kernel; however, by extending the concept to the third dimension (19,20).

Simulations

In order to examine the effects of the noise enhancement in non-Cartesian GRAPPA, a simulated PROPELLER dataset was constructed. To this end, a standard Shepp–Logan phantom was employed with a simulated eight-element one-ring head coil array where sensitivities were derived using an analytic integration of the Biot–Savart equations. The Cartesian data were resampled as PROPELLER data (8 blades, 32 phase encoding steps per blade and 128 readout points, base matrix of 128 × 128) by sinc interpolation and normal complex noise were applied to the PROPELLER *k*-space data. Accelerated (R = 2, 3, and 4) PROPELLER acquisitions were mimicked by uniformly removing not required *k*-space lines in each blade. For GRAPPA reconstruction each blade was reconstructed separately and finally gridded to a Cartesian grid using INNG (21).

G-factor Calculation from an Image Series

Recently, the pseudomultiple-replica SNR measurement method using bootstrapped statistics (10) has been introduced as a powerful method for accurate estimation of nonuniform image SNR and therefore serves here as the gold standard method.

A fully encoded image and an extra noise-only image (no RF pulse) were acquired for both the phantom and in vivo measurements. From these acquisitions a series of 300 images/volumes were artificially generated by randomly reordering the noise in the noise-only image multiple times for each receiver channel separately. After this procedure the artificial noise data are added to the fully encoded image to arrive at the artificially generated fully encoded image series. In order to generate a series of GRAPPA images, acceleration was mimicked by simply removing not required phase encoding steps for each image in the series. GRAPPA reconstructions were then performed on each image in the series. The SNR for both scenarios was calculated by evaluating the mean and standard deviation of the signal intensities through the stack of

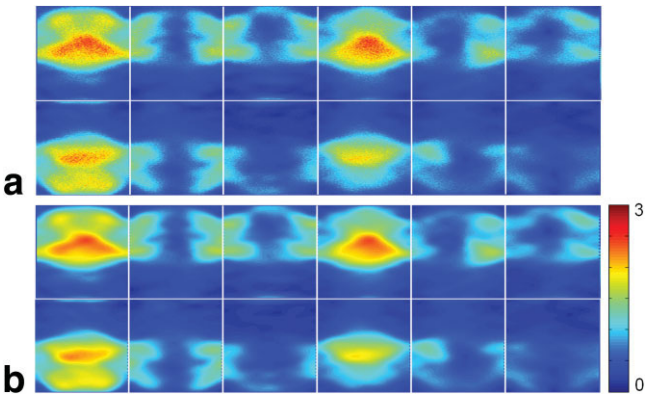

FIG. 3. Quantitative g-factor maps for uncombined GRAPPA images (R = 3, 12 channel head array) derived from **(a)** pseudomultiple replica images series derived from a phantom and extra noise scan and **(b)** directly from the GRAPPA reconstruction weights.

images on a pixel-by-pixel basis. The spatially variant noise enhancement after GRAPPA reconstruction (reference GRAPPA g-factor) is then calculated according to Eq. [9] for both the single coil images and SOS combined images.

G-factor Estimation from GRAPPA Weights

In contrast to the reference method described above, the GRAPPA g-factor estimation proposed in this work can be extracted directly from the GRAPPA reconstruction weights. In addition to the GRAPPA weights, knowledge of the noise correlations between the individual receiver channels is required, which can be derived from an additional noise scan. The GRAPPA reconstruction weights are derived from ACS data in *k*-space (see Fig. 1) and afterwards transformed into the image domain (see Fig. 2). As stated above, the g-factor maps can be calculated for each coil separately according to Eq. [10] and for SOS-combined or B1 normalized combined images according to Eq. [12]. The latter case requires an additional knowledge of the coil combination parameter $\mathbf{p}$, which can be extracted from the low-resolution ACS data or from the high-resolution reconstructed GRAPPA images themselves.

RESULTS

In order to demonstrate and validate the accuracy of the g-factor estimation presented in this work Fig. 3 provides quantitative g-factor maps for each coil image of accelerated (R = 3) GRAPPA reconstructions using (Fig. 3a) the pseudomultiple replica method and (Fig. 3b) the proposed strategy using the GRAPPA reconstruction weights.

In order to demonstrate that the quantitative g-factor estimation described here is also applicable to combined GRAPPA images g-factor maps of SOS-combined GRAPPA reconstructions (R = 4) calculated from (Fig. 4a) the pseudomultiple replica gold standard method and (Fig. 4b) the proposed strategy using the GRAPPA reconstruction weights are depicted. In addition, the g-factor map calculated without taking the noise correlations into account (Fig. 4c) is displayed. While the g-factor map in Fig. 4b perfectly matches the reference g-factor derived from the image series (Fig. 4a), the g-factor map in Fig. 4c significantly diverges from the actual g-factor due to the lack of noise correlations. The coil combining coefficients were derived from the reconstructed GRAPPA images itself.

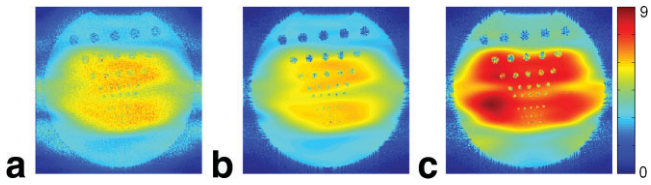

FIG. 4. Quantitative R = 4 SOS-combined GRAPPA g-factor maps derived from **(a)** pseudomultiple replica image series and **(b)** directly from the GRAPPA reconstruction weights including noise correlations and **(c)** neglecting noise correlations.

The g-factor calculation presented here allows one to calculate GRAPPA g-factors at various reduction factors. In Fig. 5 quantitative GRAPPA g-factor maps derived according to the proposed method at reduction factors of R = 2, 3, 4 and the corresponding reconstructed GRAPPA images are displayed. The expected increase of noise with increasing acceleration can be appreciated.

Besides the quantitative evaluation of GRAPPA reconstruction performance at different image accelerations, the proposed method allows a direct comparison with other reconstruction methods at the same image acceleration. To this end the quantitative noise enhancement after SENSE and GRAPPA was calculated at a reduction factor of R = 3. In Fig. 6 the g-factor maps and corresponding reconstruction results for (Fig. 6a) SENSE and (Fig. 6b) GRAPPA are displayed. While the SENSE shows the characteristic sharp edges in the g-factor map, the GRAPPA g-factor provides a more continuously varying behavior, although overall performance is virtually the same in this example.

In order to demonstrate that GRAPPA g-factors can also be derived using in vivo datasets and for 2D accelerated imaging in 3D experiments, reconstruction results and corresponding g-factor maps of conventional rectangular (R =

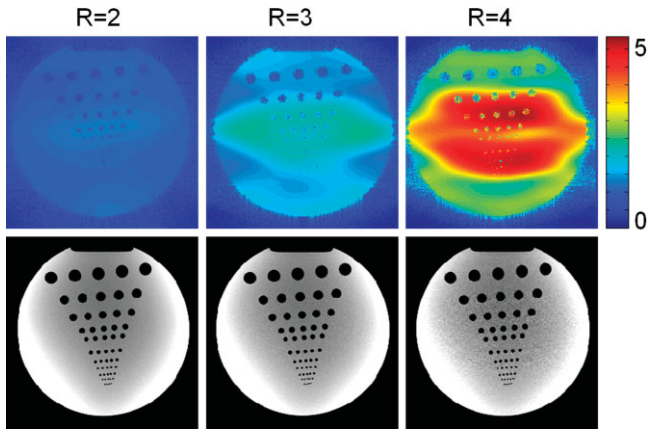

FIG. 5. Quantitative GRAPPA g-factor maps at various reduction factors R = 2, 3, 4 (top row) and corresponding SOS-combined GRAPPA reconstructions (bottom row).

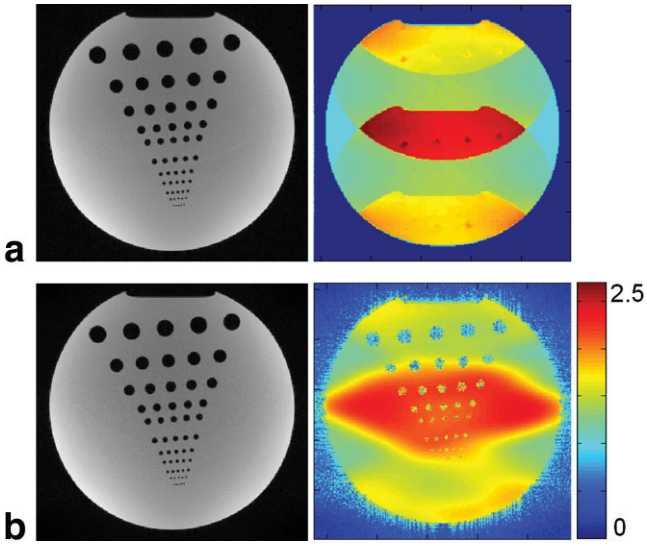

FIG. 6. Comparison between SENSE and GRAPPA reconstruction performance at a reduction factor R = 3. In **(a)** the SENSE reconstruction and corresponding g-factor map is displayed. In **(b)** the GRAPPA reconstruction and corresponding SOS-GRAPPA g-factor is displayed.

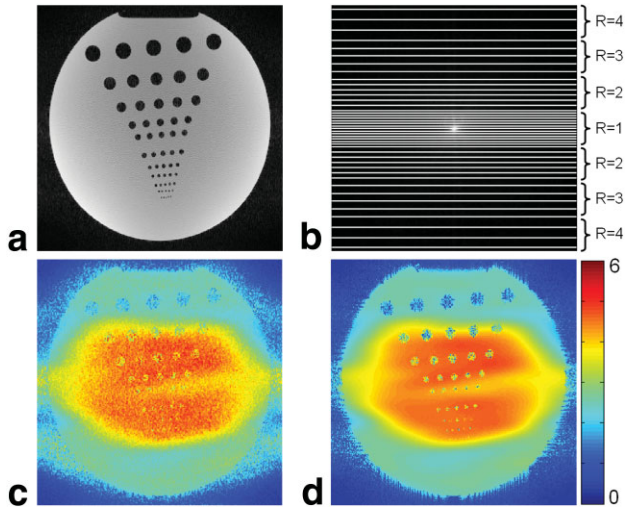

FIG. 8. Variable density acquisition with an effective reduction factor of R = 2.18. **a:** VD-GRAPPA reconstruction. **b:** VD acquisition scheme. **c:** G-factor map calculated from pseudomultiple replica series. **d:** GRAPPA g-factor map derived directly from the GRAPPA reconstruction weight sets (R = 1, 2, 3, 4).

2 × 2) and 2D CAIPIRINHA-type (R = 2 × 2(1)) acquisition (16) are displayed for the central sagittal partition in Fig. 7. The improved performance of 2D CAIPIRINHA compared to conventional rectangular 2D phase encoding can be appreciated in both (Fig. 7a) the reconstructed GRAPPA images and (Fig. 7b) the corresponding quantitative g-factor maps.

The feasibility of the g-factor estimation of multikernel GRAPPA reconstructions is demonstrated on a Cartesian variable density (VD) dataset. This dataset was artificially created as depicted schematically in Fig. 8b with areas of different acceleration factors in different *k*-space regions (R = 2, 3, or 4) and a fully sampled (R = 1) *k*-space center, resulting in an effective reduction factor of R = 2.18. The GRAPPA reconstruction was performed by applying different weight sets to the appropriate *k*-space locations. The corresponding g-factor was calculated using the reference method (Fig. 8a) and according to the proposed concept using a weighted sum of variance contributions in Eq. [12] (Fig. 8b). In addition, the GRAPPA reconstruction result is displayed (Fig. 8d).

Finally, in order to prove the applicability of the g-factor approach to non-Cartesian GRAPPA, accelerated PROPELLER experiments were simulated (R = 2, 3, and 4). For each case, quantitative g-factor maps were derived separately for each individual blade. Thereafter, the resulting single blade g-factors were rotated according to their rotation angle in *k*-space and finally combined employing Eq. [13]. In Fig. 9 the reconstruction results from (Fig. 9a) the fully encoded and (Fig. 9b) the R = 4 accelerated PROPELLER experiment are shown. The PROPELLER g-factor map is displayed in Fig. 9d and compared to the g-factor map derived from the multiple pseudoreplica SNR measurement (Fig. 9c).

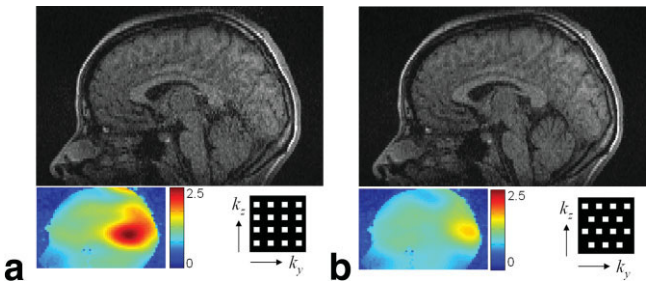

FIG. 7. Central partition in the sagittal orientation of a 4-fold accelerated 3D MPRAGE experiment after **(a)** rectangular (R = 2 × 2) and **(b)** CAIPIRINHA-type (R = 2 × 2(1)) acquisition with sampling positions shifted with respect to each other. Displayed are the SOS-combined GRAPPA reconstructions, the corresponding GRAPPA g-factor maps, and 2D phase encoding schemes.

DISCUSSION

The mathematical framework presented here allows a practical, fast, and robust quantification of the nonuniform noise enhancement in GRAPPA reconstructions for both uncombined and combined images. The results presented here are in excellent agreement with the g-factor maps derived using the pseudomultiple replica SNR measurement (10,11), which can be considered the gold standard method. Thus, quantitative GRAPPA g-factor maps can be calculated directly from the GRAPPA reconstruction weights, which are typically derived from a low-resolution scan, which can be of arbitrary image contrast (22).

It is important to note that even in the case of combined images no explicit knowledge of the coil sensitivities is required for accurate g-factor estimation. Since the GRAPPA g-factor is calculated in relation to the fully encoded image, SNR on a pixel by pixel basis the g-factor for SOS combined images are virtually identical to the g-factors employing image combinations toward uniform

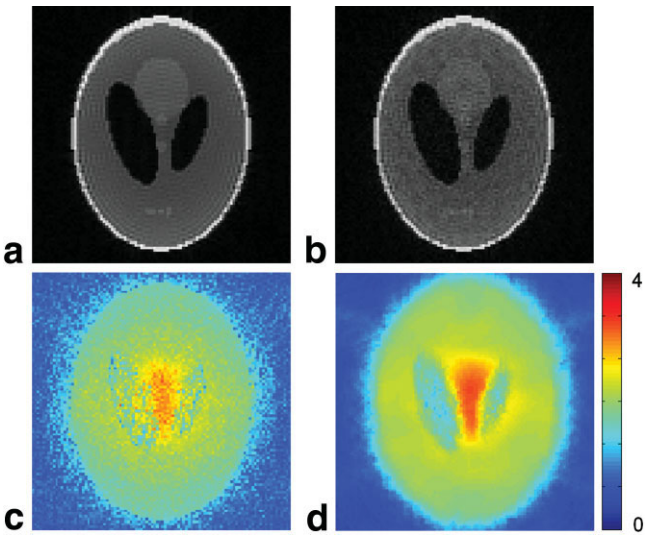

FIG. 9. Reconstruction results from **(a)** an accelerated (R = 4) simulated PROPELLER acquisition and **(b)** the fully sampled reference PROPELLER image (8 blades, 32 phase encoding lines per blade). **c:** G-factor map calculated from pseudomultiple replica series. **d:** GRAPPA g-factor map derived by calculating the g-factor for each blade separately according to Eq. [12] followed by a weighted combination of the single blade g-factors according to Eq. [13].

sensitivity or uniform noise distribution. One major advantage of the proposed strategy is that it allows one to quantitatively estimate the noise enhancement prior to the actual GRAPPA reconstruction and thus can be used to identify the optimal reconstruction kernel (number of source points, maximum possible/acceptable acceleration, regularization parameter, etc.) given a certain receiver array geometry. However, the results presented here emphasize the importance of accounting for potential noise correlations between the individual receiver channels in the calculation for accurate g-factor estimation (see Fig. 4).

In addition to kernel optimization, the GRAPPA g-factor can be used for a quantitative comparison of parallel imaging performance between different acquisition strategies such as, for example, rectangular and 2D CAIPIRINHA-type acceleration. Finally, as an extra benefit this concept allows a quantitative comparison of reconstruction performance of different parallel imaging reconstruction strategies, such as GRAPPA, SENSE, and SMASH. It has been demonstrated that quantitative g-factor maps for GRAPPA reconstructions can be derived that are similar to the g-factor maps for SENSE reconstructions. Since SENSE is considered the parallel imaging reconstruction method providing optimal SNR, the GRAPPA g-factors derived here indicate that GRAPPA indeed represents a near-optimal image reconstruction.

Besides the quantitative assessment of noise enhancement in Cartesian GRAPPA employing only one kernel, the framework presented here can be extended to acquisitions were multiple GRAPPA kernels are used as required, for example, in variable density GRAPPA (12) or non-Cartesian GRAPPA, such as radial (13), spiral (14,15), or PROPELLER acquisitions. Since only the fraction of *k*-space that has been reconstructed with a certain kernel and not the location in *k*-space matters for the noise propagation, the image variance can be calculated for each kernel separately and then weighted accordingly. Each time when a certain weight set is applied in *k*-space the noise originating from the source points propagates into the reconstructed point(s), respectively, in the image space according to its g-factor. Acquired points may be used several times even in the case of only one kernel (e.g., 4 × 3 kernel = 12 times) to calculate different missing points. The noise in the source points in the kernel region is uncorrelated for each kernel application. For this reason the noise propagation is independent of borders between regions of different GRAPPA kernels and therefore allows one to calculate the contribution of each individual kernel g-factor by counting the number of times a certain kernel has been applied in *k*-space independent of the fact that individual kernels shared the same source points. In order to validate this concept of g-factor map calculation with multiple kernels, an accelerated Cartesian variable density acquisition has been mimicked and corresponding g-factor maps were calculated. This example inherently implies the case when the ACS data is included in the final image after GRAPPA reconstruction. It is important to note that in such cases the g-factor not only reflects the coil encoding performance but also becomes dependent on the acquisition strategy.

In addition, as a proof of principle the applicability of the g-factor approach to non-Cartesian GRAPPA has been validated by presenting g-factor results of a simulated R = 4 accelerated PROPELLER acquisition which has been shown to be in good agreement with the gold standard pseudomultiple replica method. In future work the applicability to more complex non-Cartesian GRAPPA reconstructions such as radial or spiral GRAPPA need to be investigated.

Recently, a generalized pseudo-Cartesian GRAPPA reconstruction method for arbitrary trajectories has been proposed (16) which uses the GRAPPA operator gridder (GROG) (23) to shift the undersampled non-Cartesian data points to their nearest Cartesian locations followed by a Cartesian multiple kernel GRAPPA reconstruction and therefore is expected to be a perfect candidate for generalized g-factor estimation.

CONCLUSION

In this work a general framework for estimating the non-uniform noise enhancement in Cartesian GRAPPA reconstructions is presented. The GRAPPA g-factors can be derived directly from the reconstruction weights themselves for both uncombined and combined images. The proposed strategy provides a fast and powerful tool for identifying the optimal GRAPPA reconstruction parameters and for optimizing the sampling strategy for a given coil configuration and acceleration factor prior to the actual GRAPPA reconstruction. Most important, the performances of different reconstruction kernels and regularization strategies can be quantitatively evaluated. In addition, the GRAPPA g-factor enables a direct comparison of image quality between SENSE and GRAPPA reconstructions for a given application.

ACKNOWLEDGMENT

The authors thank Phillip Beatty for helpful discussions.

REFERENCES

1. Roemer PB, Edelstein WA, Hayes CE, Souza SP, Mueller OM. The NMR phased array. Magn Reson Med 1990;16:192–225.
2. Pruessmann KP, Weiger M, Scheidegger MB, Boesiger P. SENSE: sensitivity encoding for fast MRI. Magn Reson Med 1999;42:952–962.
3. Sodickson DK, Manning WJ. Simultaneous acquisition of spatial harmonics (SMASH): fast imaging with radiofrequency coil arrays. Magn Reson Med 1997;38:591–603.
4. Griswold MA, Jakob PM, Heidemann RM, Nittka M, Jellus V, Wang J, Kiefer B, Haase A. Generalized autocalibrating partially parallel acquisitions (GRAPPA). Magn Reson Med 2002;47:1202–1210.
5. Sodickson DK, Griswold MA, Jakob PM, Edelman RR, Manning WJ. Signal-to-noise ratio and signal-to-noise efficiency in SMASH imaging. Magn Reson Med 1999;41:1009–1022.
6. Kellman P, McVeigh ER. Image reconstruction in SNR units: a general method for SNR measurement. Magn Reson Med 2005;54:1439–1447 [erratum: Magn Reson Med 2007;58:211–212].
7. Yeh EN, McKenzie CA, Ohliger MA, Sodickson DK. Parallel magnetic resonance imaging with adaptive radius in k-space (PARS): constrained image reconstruction using k-space locality in radiofrequency coil encoded data. Magn Reson Med 2005;53:1383–1392
8. Wang J, Zhang B, Zhong K, Zhuo Y. Image Domain Based Fast GRAPPA Reconstruction and relative SNR degradation Factor. In: Proc 13th Annual Meeting ISMRM, Miami; 2005:2428.
9. Griswold MA. Advanced k-space techniques. 2nd Workshop on parallel MRI 2004; p 16.
10. Robson PM, Grant AK, Madhuranthakam AJ, Lattanzi R, Sodickson DK, McKenzie CA. Universal approach to quantification of SNR and g-factor for parallel MRI. In: Proc 15th Annual Meeting ISMRM, Berlin; 2007:1747.
11. Riffe MJ, Blaimer M, Barkauskas KJ, Duerk, JL, Griswold MA. SNR estimation in fast dynamic imaging using bootstrapped statistics. In: Proc 15th Annual Meeting ISMRM, Berlin; 2007;1879.
12. Heidemann RM, Griswold MA, Seiberlich N, Nittka M, Kannengiesser SAR, Kiefer B, Jakob PM. A fast method of 1D non-Cartesian parallel imaging using GRAPPA. Magn Reson Med 2007;57:1037–1046.
13. Griswold MA, Heidemann RM, Jakob PM. Direct parallel imaging reconstruction of radially sampled data using GRAPPA with relative shifts. In: Proc 11th Annual Meeting ISMRM, Toronto; 2003:2349.
14. Heidemann RM, Griswold MA, Seiberlich N, Kruger G, Kannengiesser SA, Kiefer B, Wiggins G, Wald LL, Jakob PM. Direct parallel image reconstructions for spiral trajectories using GRAPPA. Magn Reson Med 2006;56:317–326.
15. Heberlein K, Hu X. Auto-calibrated parallel spiral imaging. Magn Reson Med 2006;55:619–625.
16. Seiberlich N, Breuer F, Heidemann R, Blaimer M, Griswold M, Jakob P. Reconstruction of undersampled non-Cartesian data sets using pseudo-Cartesian GRAPPA in conjunction with GROG. Magn Reson Med 2008; 59:1127–1137.
17. Brau AC, Beatty PJ, Skare S, Bammer R. Comparison of reconstruction accuracy and efficiency among autocalibrating data-driven parallel imaging methods. Magn Reson Med 2008;59:382–395.
18. Breuer FA, Blaimer M, Mueller MF, Seiberlich N, Heidemann RM, Griswold MA, Jakob PM. Controlled aliasing in volumetric parallel imaging (2D CAIPIRINHA). Magn Reson Med 2006;55:549–556.
19. Breuer FA, Blaimer M, Seiberlich N, Griswold MA, Jakob PM. A 3D GRAPPA algorithm for volumetric parallel imaging. In: Proc 14th Annual Meeting ISMRM, Seattle; 2006:286.
20. Blaimer M, Breuer FA, Mueller M, Seiberlich N, Ebel D, Heidemann RM, Griswold MA, Jakob PM. 2D-GRAPPA-operator for faster 3D parallel MRI. Magn Reson Med 2006;56:1359–1364.
21. Moriguchi H, Duerk JL. Iterative Next-Neighbor Regridding (INNG): improved reconstruction from nonuniformly sampled k-space data using rescaled matrices. Magn Reson Med 2004;51:343–352.
22. Breuer FA, Blaimer M, Mueller MF, Seiberlich N, Heidemann RM, Griswold MA, Jakob PM. Autocalibrated parallel imaging with GRAPPA using a single prescan as reference data. In: Proc ESMRMB 2004:398.
23. Seiberlich N, Breuer FA, Blaimer M, Barkauskas K, Jakob PM, Griswold MA. Non-Cartesian data reconstruction using GRAPPA operator gridding (GROG). Magn Reson Med 2007;58:1257–1265.